



ON 3D-BEAMFORMING IN THE WIND TUNNEL

Dirk Döbler¹, Jörg Ocker², Dr. Christof Puhle¹

¹GFaI e.V., Volmerstraße 3, 12489 Berlin, Germany

²Dr. Ing. h.c.F. Porsche AG, 71287 Weissach, Germany

ABSTRACT

Especially in the early development stages a quick and reliable ranking and rating of aero-acoustic sound sources is important to fulfil the challenging requirements the engineers face. For a localization and detailed analysis of these aero-acoustic sources, a complex measurement system consisting of three separate microphone arrays was installed in the Porsche aero-acoustic wind tunnel [1]. All arrays are mounted in a reinforced framework positioned out-of-flow at the smallest possible distance to the test object. The common evaluation technique for the recorded microphone data is known as “acoustic camera principle” or beamforming: acoustic source maps produced by certain beamforming algorithms are mapped on a 2-dimensional optical image. Moreover, it is feasible to map the beamforming results on a 3-dimensional model of a car. This paper is about the challenges encountered in the 3D-approach and how these were coped. In particular, we consider the calibration of the microphone and array positions, the influence of the focus on the 2D-mapping and the problem merging the information of all three arrays in 3D-beamforming.

1 INTRODUCTION

The new Porsche wind tunnel can be operated up to velocities of 300 km/h. Due to its very low background noise level, microphone arrays are suitable for the localization and precise evaluation of sound sources. The Porsche wind tunnel microphone array system was developed and built in cooperation with GFaI e.V. and gfai tech GmbH, Berlin and installed in January 2015.

1.1 Array hardware

The system consists of three identical microphone arrays of dimension 5 m x 3 m, each equipped with 192 electret microphones and an integrated Full-HD camera. In order to achieve a high localization accuracy of acoustic sources, each differentially transmitted channel can be sampled up to a frequency of 192 kHz. All 576 channels work synchronously, hence it is feasible to combine the data of all three arrays to form one “super array”.

A (repeatable) positional accuracy of ± 1 mm is ensured for each of the arrays. This precision is met even at the maximum wind speed due to the high stability and the low weight of the arrays resulting from a special sandwich construction integrated in a lightweight reinforced frame (see Fig. 1 and Fig. 2).

The relative microphone positions of each array were determined using the ADECO method [2]. Since the knowledge of the absolute microphone positions is critical to the final 3-dimensional beamforming result, the remaining question was: How can we identify the orientation and location of the microphone arrays with respect to each other? We will address this question in section 2.



Fig. 1: Framework in measurement position, microphone arrays in parking position

Fig. 2: Framework and microphone arrays in measurement position

1.2 3D-Beamforming for better results

Typically, the result generated by one microphone array, the acoustic source map, is overlaid to a 2-dimensional optical image. In total, three photos are created for each measurement: one from the driver's side (left array), one from the passenger's side (right array) and one from above. For this 2D-approach, the array layout and calculation methods such as shear-layer correction, cross-spectral matrix, diagonal removal, CLEAN-SC and corresponding first results were presented in [3]. Two examples are shown in Fig. 3 and 4.

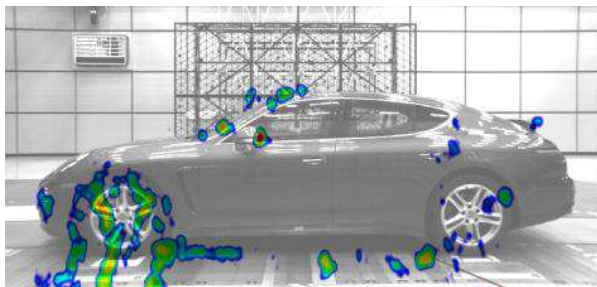


Fig. 3: 2D-Map Panamera S, 1,6 kHz, CLEAN-SC, 25 dB dynamic, driver's side

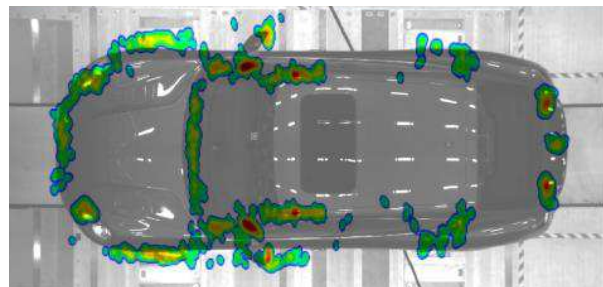


Fig. 4: 2D-Map Panamera S, 1,6 kHz, CLEAN-SC, 25 dB dynamic, from top

However, for 3D-structured objects, 3D-beamforming can offer more accuracy in source localization and determination of source strengths in the acoustic map [4]. This is motivated even further by our discussion of the focus dependency of the 2D-approach in section 3. Eventually, we present our 3D-beamforming approach in section 4.

2 MULTIPLE 3D-ARRAY CALIBRATION

To render 3D-beamforming possible, a sample synchronous recording is not the only requirement. An exact knowledge of the orientation and location of the arrays in addition to the microphone coordinates of each array is also important. For this purpose, the ADECO algorithm introduced in [2] was extended. In the first step, we determined the relative microphone positions of each array by applying standard ADECO. Then, also following the idea of [2], we performed an additional measurement recording the signals of all three arrays simultaneously. The source was a spark generator which generated a large number (approx. 100-200) of point sources at various locations within the area of the vehicle measurements. Synchronized with the measurements of the arrays, the electric signal of the spark generator was recorded as well. In the analysis of this measurement, the positions of the temporally well-known sound sources are assumed to be randomly distributed, and the microphone positions are initialized with the coordinates obtained before arranging the arrays indiscriminately to each other (see Fig. 5). In the next step, the positions of the sound sources relative to each array are determined using the fitting procedure of [2] (see Fig. 6). Then, one system (sound sources and their associated array) is defined as the reference system. Finally, the other two systems are rotated and shifted to match all corresponding sound sources (see Fig. 7). This technique determines the relative position of the arrays to each other and ensures that all three arrays map a sound source at the same spatial position.

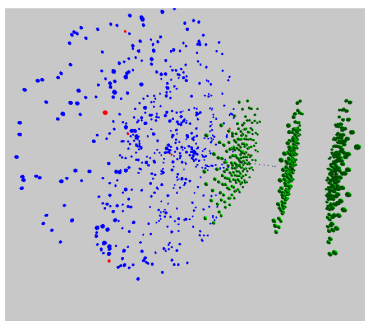


Fig. 5: Initial configuration, microphone arrays (green balls), random source positions (blue/red balls), discarded data (red balls)

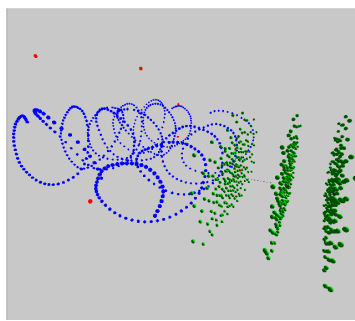


Fig. 6: Determined source positions and their associated microphone arrays

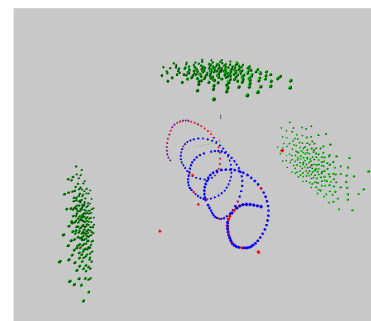


Fig. 7: Determined array positions

In order to validate the precision of this procedure, a final measurement using the spark generator method was performed in the area of vehicle measurements. Now, the three main lobes of the arrays were visualized in one cubic point cloud (cf. Fig. 8, 9 and 10). Using this method, it could be concluded that the maximal deviation from the source position is 5 mm. This is within the expected accuracy of the complete system.

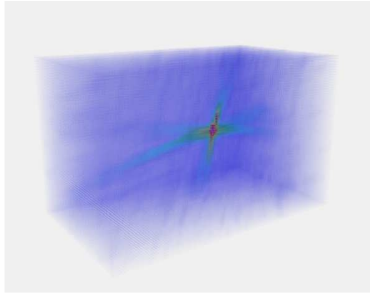


Fig. 8: Mainlobes from right, left and top array, illustrated in a cubic ($0.3\text{ m} \times 0.2\text{ m} \times 0.2\text{ m}$) point cloud

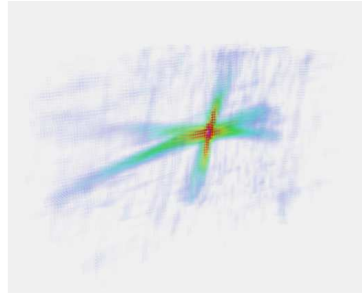


Fig. 9: Mainlobes in a cubic point cloud ($0.15\text{ m} \times 0.1\text{ m} \times 0.1\text{ m}$)

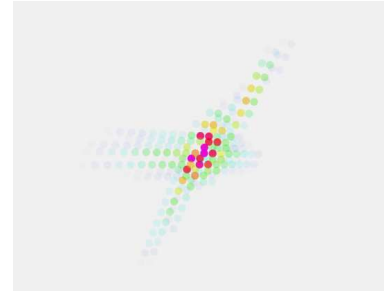


Fig. 10: Mainlobes in a cubic point cloud, pixel size 1 mm

3 FOCUS DEPENDENCY

A simulation of the decrease in source strength caused by an erroneous distance of the 2D-beamforming plane (focus) is evaluated in Fig. 11. For example, a focus deviation of 300 mm leads to an error in the mapped source strength up to 9.5 dB depending on the frequency under consideration. 300 mm is the typical distance from the outmost edge of a side-view mirror to its root.

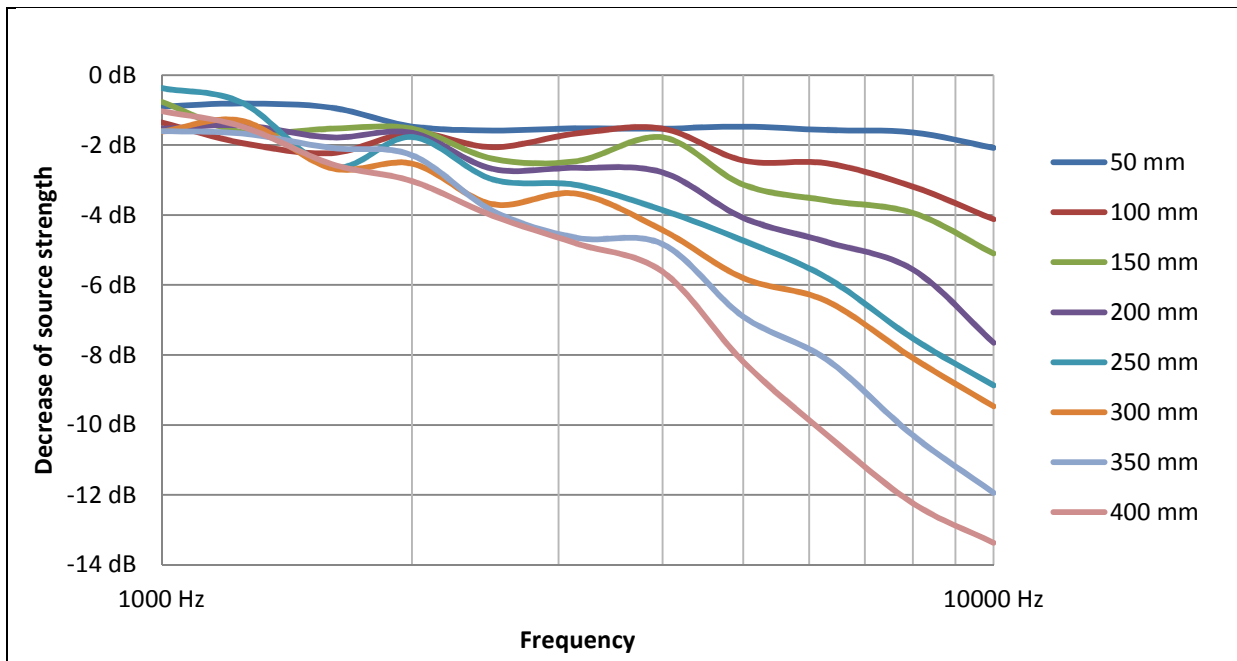


Fig. 11: Source strength in relation to focus deviation and frequency, array $5\text{ m} \times 3\text{ m}$, source distance from array 3.5 m

Another important factor when investigating the influence of the focus is the erroneous localization of the sources in the map. Fig. 12 visualizes the source localization error in relation to the focus error for a source simulated at a position 1 m off the array center. For example, a focus deviation of 200 mm causes an error in the localization of this source up to 100 mm. For sources on a side-view mirror, this error is unacceptable.

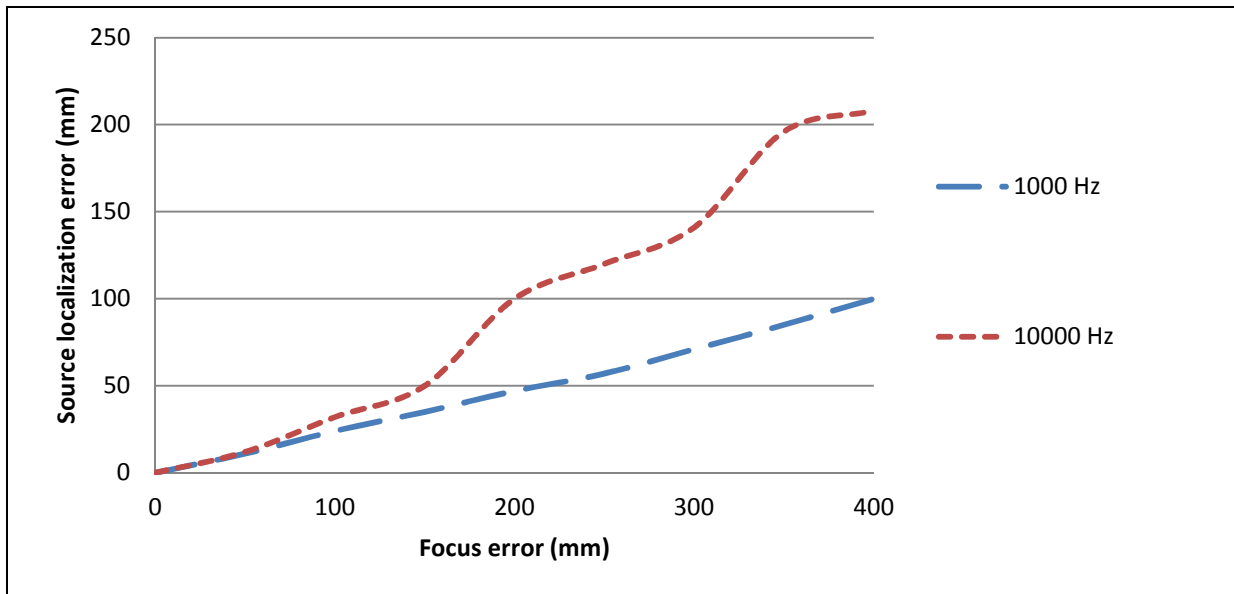


Fig. 12: Source localization error, array 5 m x 3 m, source distance from array 3.5 m

Finally, the available array dynamic (the difference between main lobe and side lobes) decreases dramatically in case of a focus error, especially for higher frequencies. Fig. 13 quantifies this effect for a focus deviation of 400 mm.

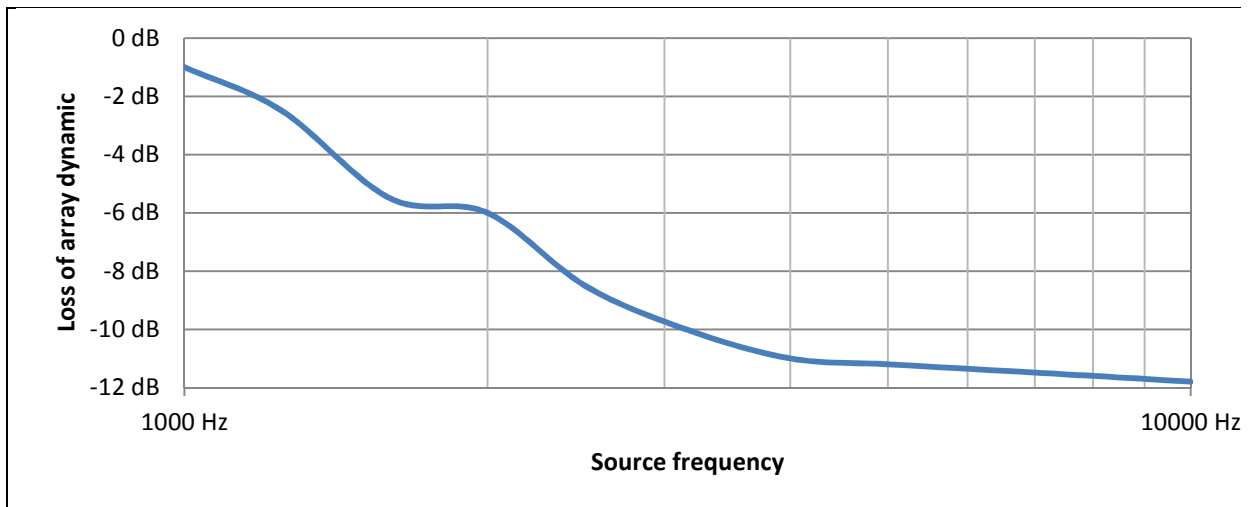


Fig. 13: Loss of array dynamic, focus error 400 mm

These facts together with the distinct visualization of sources motivate a 3-dimensional approach.

4 3D-BEAMFORMING

With the given hardware, two approaches are conceivable: the combination of all three arrays in order to form one "super array" or the generation of three separate maps together with a merging procedure onto one 3D-model.

4.1 Combining all three arrays into one array

The simplest idea of merging the microphone information of all three arrays is to treat them as one array. However, there are several flaws to this approach. First of all, the resulting array is not optimized in comparison to the highly optimized individual arrays. This might lead to unfavourable point spread functions and to a very shallow depth of field. These effects are even worsened by incorporating the concept of visibility, since the subset of visible microphones varies over the map points. Moreover, these visibilities introduce the problem of normalizing the sound pressures at each map point.

4.2 Separate computations and merging of maps

A more evolved approach of combining the microphone information of all three arrays is to compute a map for each individual array and merge the resulting maps. On the one hand, this takes advantage of the optimized point spread functions and the depth of field of each individual array. On the other hand, this approach allows for handling the visibility on the basis of each array as a whole instead of each microphone, this remarkably reduces the normalization difficulties mentioned before.

Figure 14 and 15 visualize the array based visibility concept, points visible to the optical camera of the corresponding array are coloured blue, those invisible are coloured grey.

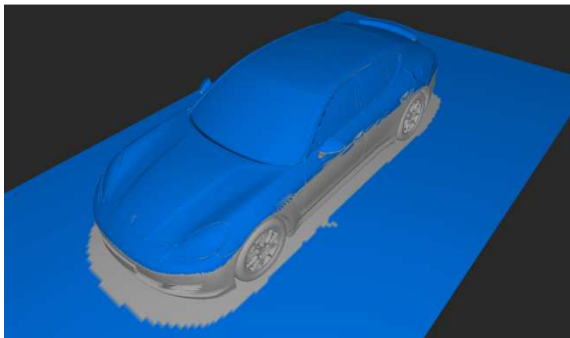


Fig. 14: 3D-Model Panamera S, Points visible from the top array (blue)

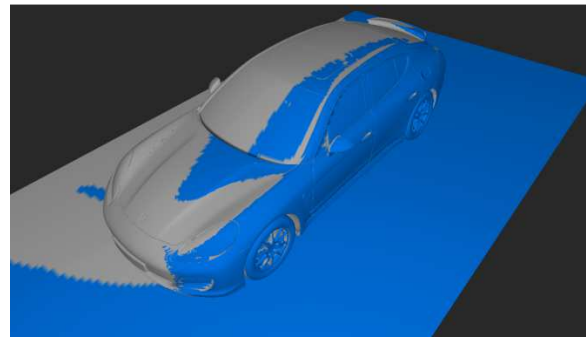


Fig. 15: 3D-Model Panamera S, Points visible from the left array (blue)

To illustrate the merging process, we compute standard beamforming maps for the visible points of both top and left array (see Fig. 16 and 17).

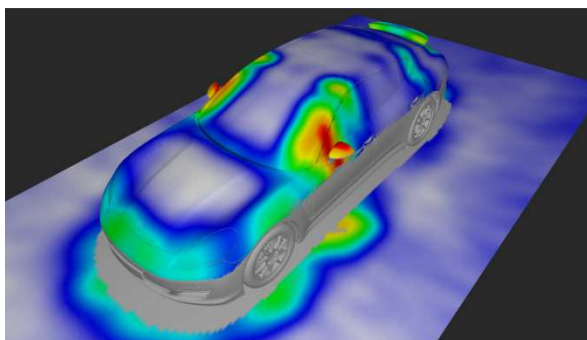


Fig. 16: 3D-Map Panamera S, 2kHz, FDBF, Points visible from the top array

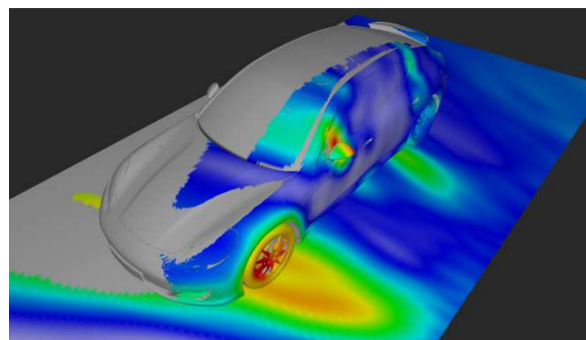


Fig. 17: 3D-Map Panamera S, 2kHz, FDBF, Points visible from the left array

To tackle the normalization problem, we compare the medians of the sound pressure levels of the points visible to every array included in the merging process and match the noise levels before averaging the corresponding maps (cf. Fig. 18 and 19).

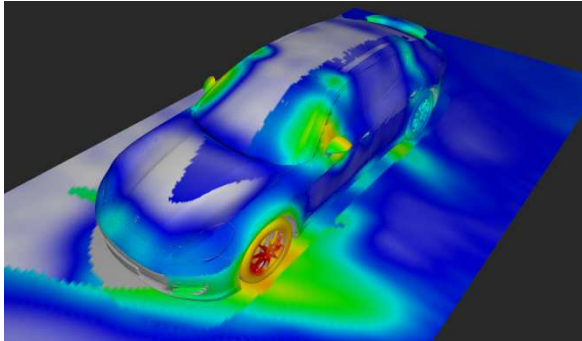


Fig. 18: Merged 3D-Map Panamera S, 2 kHz, FDBF, without normalization

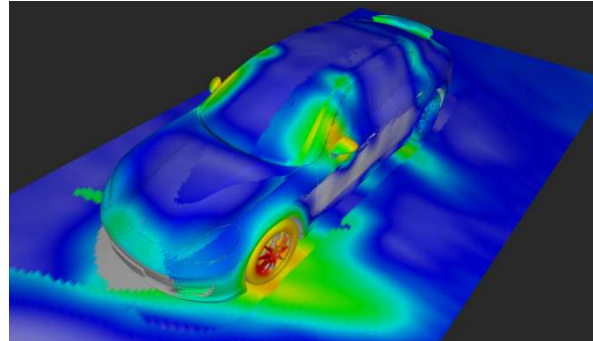


Fig. 19: Merged 3D-Map Panamera S, 2 kHz, FDBF, normalized

4.3 Deconvolution

As far as deconvolution methods are concerned, the large number of points in a 3D-model calls for a computationally efficient choice. CLEAN-SC is only twice as demanding as conventional beamforming (see [5]). Figure 20 shows an example CLEAN-SC map resulting from the approach described in section 4.2 using all three arrays.

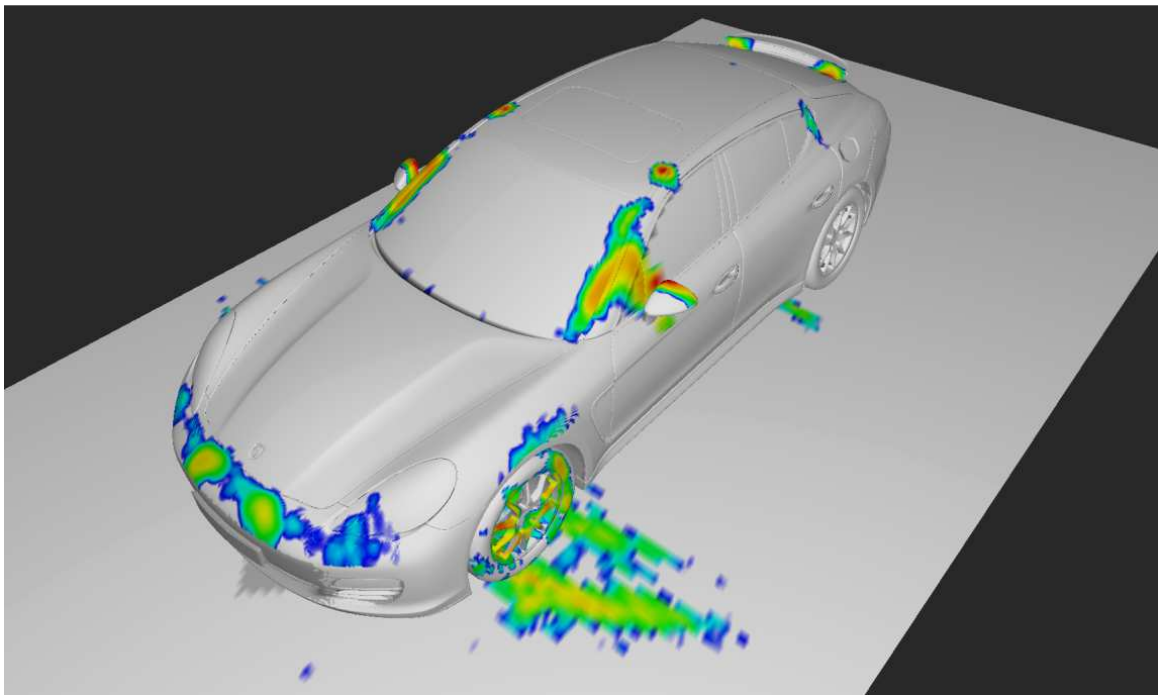


Fig. 20: Merged 3D-Map Panamera S, 2 kHz, CLEAN-SC, 38 dB dynamic

5 SUMMARY

Aero-acoustic sources have a 3-dimensional distribution. Consequently, 3D-beamforming is the method of choice in order to obtain detailed information about the sources that are generated in a wind tunnel. The calibration of the microphone and array positions of the Porsche wind tunnel microphone array system using ADECO proved to be a fast and reliable calibration method. The most suitable approach of combining the microphone information of all three arrays was to compute a beamforming map for each individual array and merge the normalized maps. For each of these maps, CLEAN-SC demonstrated to be a robust and efficient deconvolution method.

REFERENCES

- [1] H. Stumpf, P. Röser, T. Wiegand, B. Pfäfflin, J. Ocker, R. Müller, W. Eckert, H.-U. Kroß, S. Wallmann: “The new aerodynamic and aeroacoustic wind tunnel of the Porsche AG” Stuttgarter Symposium, 2015
http://www.bebec.eu/Downloads/BeBeC2008/Papers/BeBeC-2008-14_Guerin_Weckmueller.pdf, Proceedings on CD of the 2nd Berlin Beamforming Conference, 19-20 February, 2008.
- [2] D. Döbler: “Automatic detection of microphone coordinates”, BeBeC 2010 conference proceedings, Berlin, 2010.
- [3] J. Ocker, S. Tilgner: “The Porsche Wind Tunnel Microphone Array System”, Aachen Acoustic Colloquium, 2015
- [4] A. Meyer, D. Doebler: “Noise source localization within car interior using 3D microphone arrays”, BeBeC 2006 conference proceedings, Berlin, 2006
- [5] P. Sijtsma: “CLEAN based on spatial coherence”, AIAA Paper 2007-3436, 2007